

# Microstructural evolution of Y123/Ag composites during sintering

W. H. TUAN, J. M. WU

*Institute of Materials Science and Engineering, National Taiwan University, Taipei, Taiwan 10764*

The grain-growth kinetics of  $\text{YBa}_2\text{Cu}_3\text{O}_{7-x}$  (Y123) and the coarsening kinetics of silver inclusions in Y123/Ag composites during sintering were investigated. The sintering was carried out in the temperature range 900–950 °C. The addition of silver lowered the formation of a liquid phase and the grain growth of Y123 in Y123/Ag composites was thus enhanced at the beginning of sintering. However, as the effective silver content was increased, more silver inclusions became interconnected, and the grain growth kinetics and coarsening kinetics slowed down significantly. This may be due to the mass transportation paths progressively changing from the grain boundaries to interfacial boundaries as the amount of interconnected silver networks is increased. The grain growth kinetic constant was calculated and compared with other published data. Because the inclusion was ripened with the growth of matrix grains, the coarsening of silver inclusions was deduced to be a coalescence process.

## 1. Introduction

The recent discovery of high- $T_c$  ceramic superconductors [1, 2] has led to world-wide research to develop superconducting material for useful applications. The  $\text{YBa}_2\text{Cu}_3\text{O}_{7-x}$  compound, commonly known as “Y123”, has received much attention because of its high critical temperature. For most practical applications, superb mechanical properties are essential. However, previous researchers have observed that the mechanical properties of Y123 compounds are generally poor, especially the unacceptably low fracture toughness [3–5]. To improve the fracture toughness of Y123 is therefore a major research directive.

The approach of adding silver inclusions, which interact with the propagation of cracks, has been much studied [6–9]. This approach has successfully enhanced the fracture toughness of Y123 by two-three-fold. The presence of silver inclusions can affect the grain-growth kinetics of Y123 [10]. However, no detail investigation has yet been carried out on the grain-growth kinetics of Y123 in Y123/Ag composites.

Silver inclusions can also grow during sintering. The second-phase particles in ceramic compacts can ripen by two distinct processes: Ostwald ripening or coalescence. During Ostwald ripening, small particles disappear while large ones grow because of the variation of solubility with particle size. Alternatively, particles can grow by a coalescence process, if they are dragged by migrating matrix grain boundaries. In this process, grain growth and the disappearance of small matrix grains causes particles to meet, coalesce and thus form larger particles.

Because grain boundaries of Y123 not only act as possible sources for mechanical failure but are also

responsible for its low critical current [11], microstructural control during sintering is very important. In the present study, the grain-growth kinetics of Y123 containing silver inclusions, together with the coarsening kinetics of the silver inclusion, were investigated.

## 2. Experimental procedure

The Y123 powder was prepared by the solid-state reaction of the constituent oxides  $\text{Y}_2\text{O}_3$ , CuO and BaO. Powdered  $\text{Y}_2\text{O}_3$ , CuO and  $\text{BaCO}_3$  were mixed in appropriate proportions and were ball milled in ethyl alcohol for 24 h using zirconia balls as the grinding medium. The slurry was dried with a rotary evaporator. The powder mixtures were then calcined at 950 °C for 12 h, and annealed at 480 °C for 8 h in a flowing oxygen atmosphere. The calcined powder mixtures were ball milled in ethyl alcohol for 24 h. The slurry was settled for 10 min to remove hard agglomerates. The suspension was collected and dried, and after crushing they were passed through a plastic sieve with aperture size 0.074 mm. The average particle size of the resulting Y123 powder was 0.92  $\mu\text{m}$ .

The Y123/Ag composites were prepared by ball milling various amounts of  $\text{Ag}_2\text{O}$  (Johnson Matthey Material Tech., UK) with the Y123 powder for 24 h. The resulting compositions contained 5–20 vol % Ag after sintering. The powder mixtures were dried and sieved. Specimens, 1 cm diameter and 0.3–0.4 cm high, were prepared by uniaxial pressing at 200 MPa in a steel mould. The samples were sintered in a flowing oxygen atmosphere in the temperature range 900–950 °C and then annealed at 480 °C. To avoid any detrimental effect which might be generated by the decomposition of silver oxide to silver and oxygen, the

samples were heated slowly to 350 °C at a heating rate of 0.5 °C min<sup>-1</sup>, and held at that temperature for 3 h. The heating rate between 350 °C and the sintering temperature was 5 °C min<sup>-1</sup>. The cooling rates between the sintering temperature and 480 °C, and 480 °C and room temperature were 3 and 2 °C min<sup>-1</sup>, respectively.

The thermal behaviour of the powder mixtures was investigated by differential thermal analysis (DTA, DTA1600, DuPont Co., USA) in an oxygen atmosphere. The heating rate applied was 10 °C min<sup>-1</sup>. Bulk density was determined by measuring the weight and dimensions of the samples. By assuming that the reaction between Y123 and silver was limited, the relative densities of the composites were estimated by the rule of mixtures (ROM) to have a theoretical density of 6.38 g cm<sup>-3</sup> for Y123 and 10.5 g cm<sup>-3</sup> for silver. Phase identification was performed by X-ray diffractometry (Phillips PW1729, Phillips Co., The Netherlands).

The polished surfaces were prepared by polishing with 6 and 1 µm diamond particles and 0.05 µm alumina paste. The microstructure of the composites was observed by reflected polarized light microscopy. The grain size of Y123 and the silver inclusion size were determined by the linear intercept technique on colour micrographs taken from the polished sections. The interconnectivity of the silver inclusions was determined by measuring resistivity at room temperature [9].

### 3. Results

The DTA curves in Fig. 1 reveal one and four endothermic peaks for the Y123 and the mixtures of Y123 and silver oxide, respectively. The X-ray diffraction patterns of the sintered Y123/Ag composites were compared to the published patterns [12] and identified as mixtures of orthorhombic Y123 and cubic silver. The relative density of the composites containing various amounts of silver inclusions were shown to be function of sintering temperature (Fig. 2). The grain size of Y123 and the silver inclusion size in the composites in Fig. 2 are shown as a function of sintering temperature in Figs 3 and 4, respectively. The relative density of the composites containing various amounts of silver inclusions is shown in Fig. 5 as a function of sintering time at 930 °C. The grain size of Y123 and the inclusion size of silver in the composites in Fig. 5 are shown as a function of sintering time in Figs 6 and 7, respectively, and typical microstructures for the composites are shown in Fig. 8. From the resistivity measurement, the results indicate that the interconnected silver inclusions are increased with increasing effective silver content [9] which is the product of the expected silver content for fully dense composite and the relative density.

### 4. Discussion

The DTA curve in Fig. 1 indicates that the endothermic peak for Y123 is at 952 °C. This small endothermic peak is believed to be due to the generation of

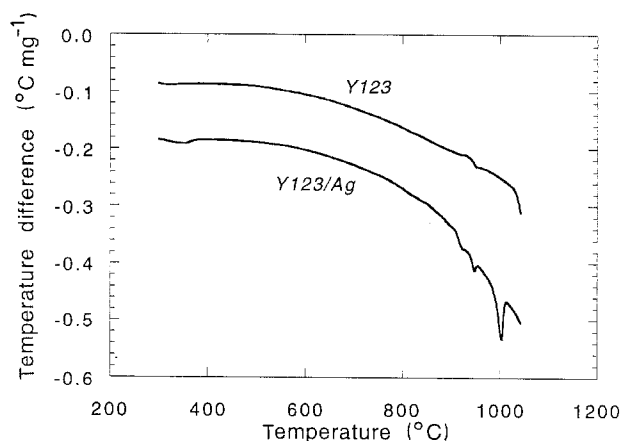


Figure 1 DTA curves for Y123 powder and powder mixtures of Y123 and silver oxide in an oxygen atmosphere.

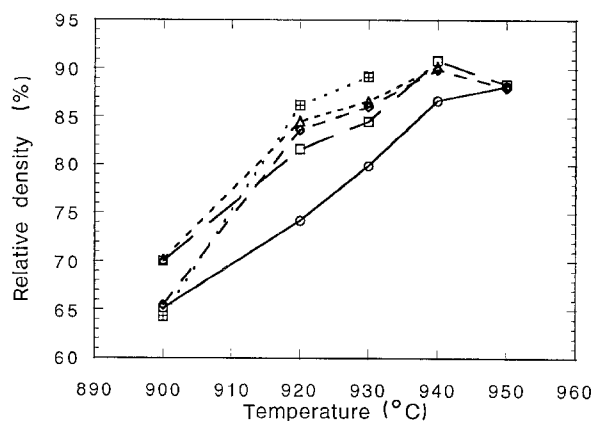


Figure 2 The relative density of the composites as a function of sintering temperature with the samples sintered at the indicated temperatures for 360 min. (○) 0% Ag, (□) 5% Ag, (◇) 10% Ag, (△) 15% Ag, (⊞) 20% Ag.

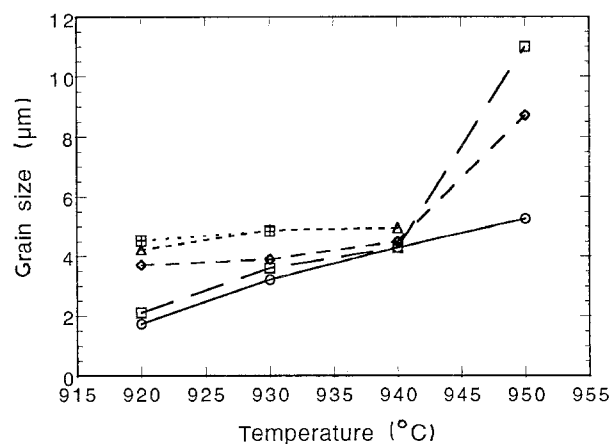


Figure 3 The grain size of Y123 in the composites as a function of sintering temperature with samples sintered at the indicated temperatures for 360 min. (○) 0% Ag, (□) 5% Ag, (◇) 10% Ag, (△) 15% Ag, (⊞) 20% Ag.

a liquid phase, possibly a Ba–Cu–O melt [11]. Such a liquid phase is commonly observed by DTA in Y123 samples whose composition is slightly rich in barium and copper. For the powder mixtures of Y123 and silver oxide, peaks were observed at 350, 921, 947 and

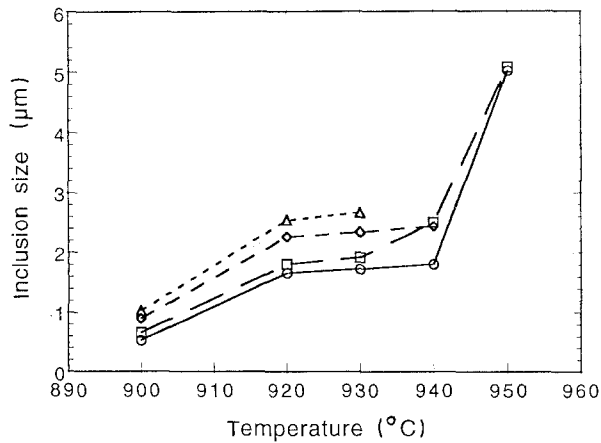


Figure 4 The size of silver inclusions in the composites as a function of sintering temperature with samples sintered at the indicated temperatures for 360 min. (○) 5% Ag, (□) 10% Ag, (◇) 15% Ag, (△) 20% Ag.

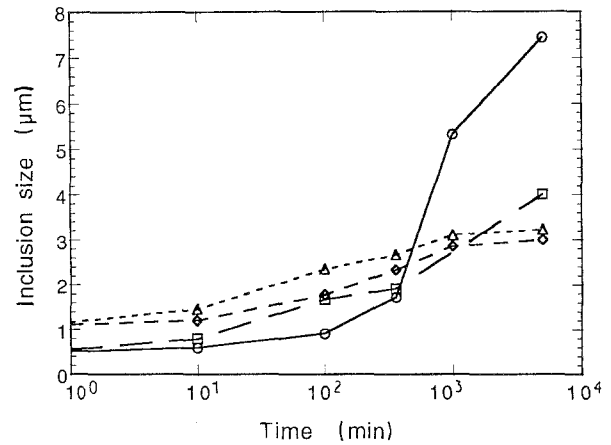


Figure 7 The size of silver inclusions in the composites as a function of sintering time at 930 °C. (○) 5% Ag, (□) 10% Ag, (◇) 15% Ag, (△) 20% Ag.

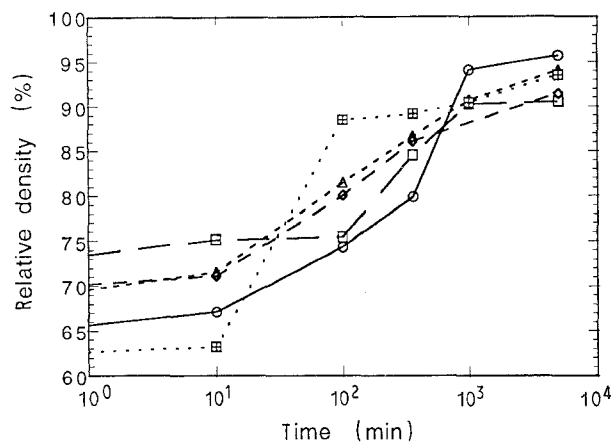


Figure 5 The relative density of the composites as a function of sintering time at 930 °C. (○) 0% Ag, (□) 5% Ag, (◇) 10% Ag, (△) 15% Ag, (⊞) 20% Ag.

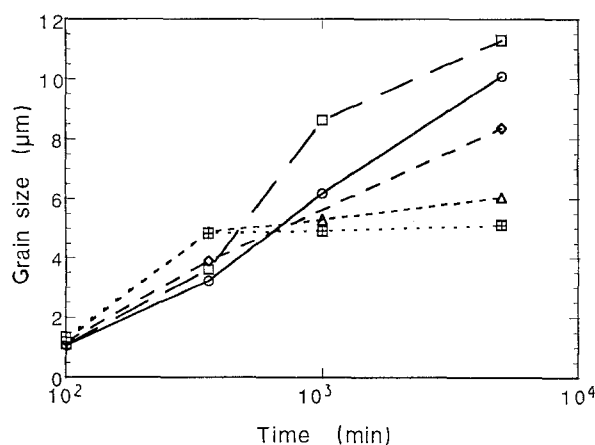


Figure 6 The grain size of Y123 in the composites as a function of sintering time at 930 °C. (○) 0% Ag, (□) 5% Ag, (◇) 10% Ag, (△) 15% Ag, (⊞) 20% Ag.

1004 °C. The first peak reveals the decomposition reaction of silver oxide to silver and oxygen. The second peak results from the liquid-phase formation of Y123. This indicates that the addition of silver accelerates the formation of the liquid phase by about

20 °C. The third peak is thought to result from the melting of silver. This suggests that for the materials used in the present study, Y123 and silver have limited mutual solubility.

From Fig. 3, for the composites sintered at the indicated temperatures for 360 min, the matrix grains grow in the presence of silver. At 950 °C the matrix grains become much larger, suggesting that the presence of the liquid phase enhances the grain growth of Y123, and the presence of silver melt further increases the grain-growth rate. From Fig. 6, for the composites, the matrix grains are seen to grow faster at the beginning of sintering at 930 °C; however, the grain-growth rate slows down as sintering time is increased.

The grain-growth kinetics depicted in Fig. 6 are analysed in terms of the relation

$$G^n - G_0^n = K(t - t_0) \quad (1)$$

where  $G$  is the grain size at time  $t$ ,  $n$  the grain-growth kinetic exponent,  $G_0$  the grain size after a short sintering time (in the present study, 100 min is taken as  $t_0$ ), and  $K$  the grain-growth constant. The values of  $n$  for Y123 have been suggested by Shin *et al.* [13] to be 4.8 from 950–990 °C, and by Chu and Dunn [14] to be 5 from 925–950 °C and 3 at 975 °C. By applying the linear regression technique to the data in Fig. 6, integer values for  $n$  ranging from 2–6 can result with nearly the same correlation factor. With this in mind, a value of  $n = 3$  was chosen to provide a basis for comparison of the values of  $K$  with other data [13, 14], Table I.  $K$  for Y123 at 930 °C is very close to that reported by Chu and Dunn [14]. However, the value is about one order larger than that reported by Shin *et al.* [13]. From the study of the grain-growth kinetics of alumina, the presence of a small amount additive, e.g. 250 p.p.m. magnesia, may decrease the grain-growth constant [15] by more than one order of magnitude. This may also be the case for Y123.

The values of  $K$  are shown as a function of silver content in Fig. 9. Owing to the presence of the liquid phase,  $K$  for 5% composites is larger than that of Y123. However, except for the composites containing 5 vol % Ag,  $K$  decreases drastically with increasing

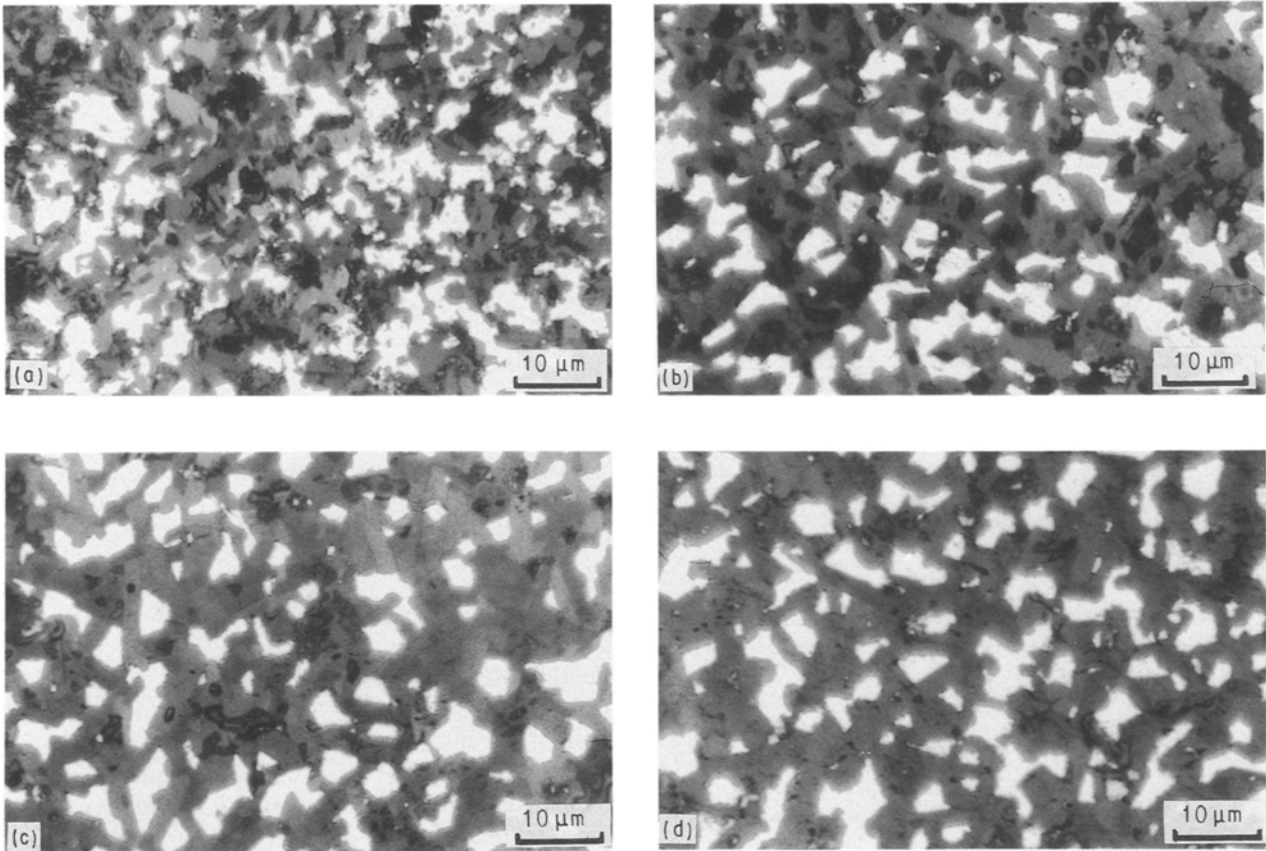


Figure 8 Typical microstructures of Y123/Ag composites. The composites contain 20 vol % silver and were sintered at 930 °C for (a) 100, (b) 360, (c) 1000 and (d) 5000 min.

TABLE I Comparison of grain-growth constants,  $K$  (cubic growth kinetics), for grain growth of Y123 in Y123 and in Y123/Ag composites

Temperature (°C)	Ag content (%)	$K$ ( $10^{-18} \text{ m}^3 \text{ min}^{-1}$ )	Reference
925	0	0.22	Chu and Dunn [14]
950	0	2.32	
975	0	5.44	
950	0	0.018	Shin <i>et al.</i> [13]
965	0	0.020	
975	0	0.020	
990	0	0.046	
930	0	0.21	Present work
930	5	0.27	
930	10	0.12	
930	15	0.021	
930	20	0.0041	

silver content. Note that the grain-growth rate exhibits a 50-fold reduction as 20 vol % silver inclusion is added, Table I. The dependence of grain-growth kinetics on sintering temperature is shown in Fig. 10; the activation energy is decreased with increasing silver content.

The inclusion size for all the composites is shown as a function of grain size in Fig. 11. The inclusion size increases with increasing grain size. Note that except at the beginning of the curve, the inclusion size is proportional to the matrix grain size and the inclusion size is smaller than the grain size. From micro-

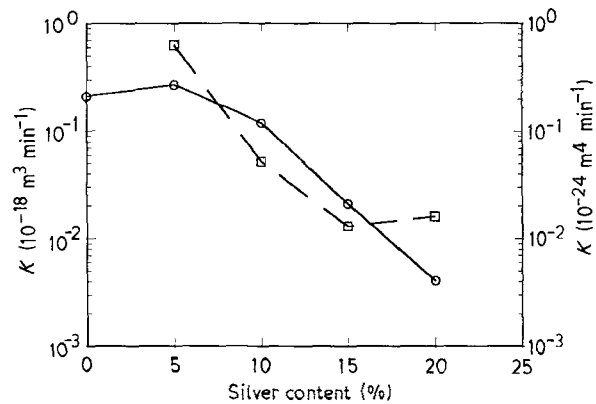


Figure 9 (○) The grain-growth constant,  $K$ , and (□) coarsening constant,  $K'$ , as a function of silver content. The samples were sintered at 930 °C.

structural observation, Fig. 8, the inclusions remain at the grain junctions throughout sintering, suggesting that the coarsening of inclusions is controlled by the migrating grain boundaries of Y123. The coarsening of inclusions is, therefore, a coalescence process, for which there is a  $t^{1/4}$  dependence [16]; this is observed for composites sintered at 930 °C. Therefore, the relationship

$$R^4 - R_0^4 = K'(t - t'_0) \quad (2)$$

can be used to describe the coarsening kinetics, where  $R$  is the inclusion size at time  $t$ ,  $R_0$  the inclusion size at  $t'_0$ , 1 min is taken as  $t'_0$ , and  $K'$  the inclusion-coarsening constant. The values of  $K'$  are shown as a function

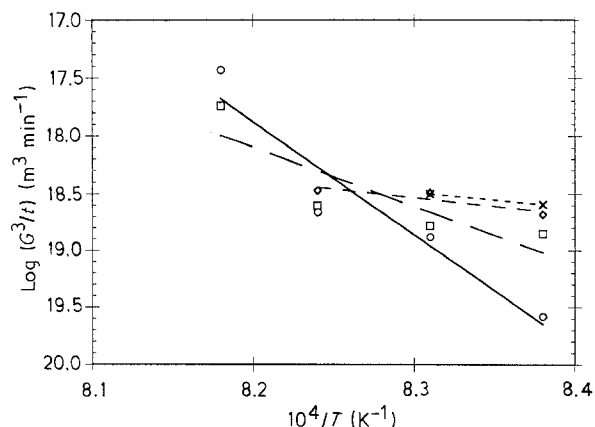


Figure 10 The grain growth constant as a function of sintering temperature. The samples were sintered at the indicated temperatures for 360 min. (○) 5% Ag, (□) 10% Ag, (◇) 15% Ag, (×) 20% Ag.

of silver content in Fig. 9; this indicates that the coarsening rate of inclusions is dramatically decreased with increasing silver content. For the 20 vol % Ag composite, the coarsening constant is 1/40th that of 5 vol % Ag composite, Table II.

The variation of coarsening of silver inclusions is shown as a function of sintering temperature in Fig. 12.  $K'$  shows a strong dependence on the formation of the liquid phase and the melting of silver. It further confirms the existence of a liquid phase above 910 °C and of a silver melt above 940 °C in the present system.

The increase in interconnected silver inclusions with increasing silver content [9], suggests that the grain-growth rate is decreased with increasing interconnectivity of silver inclusions. As two phases with limited solubility form interpenetrating microstructures, the dominant mass transporting paths are probably shifted from grain-boundary diffusion to interfacial diffusion. This can be visualized from the decrease in activation energy of grain growth as the silver content is increased, Fig. 10. A similar case can be found in the Al/Al<sub>2</sub>O<sub>3</sub> system. The activation energy for silver isotope diffusion along the Al/Al<sub>2</sub>O<sub>3</sub> interface, 177 kJ mol<sup>-1</sup>, is smaller than that of silver isotope diffusion along the grain boundary of Al<sub>2</sub>O<sub>3</sub>, 392 kJ mol<sup>-1</sup> [17]. Because the grain-growth rate slows down due to the presence of interconnected silver inclusions, it may imply that the mass transportation along the grain boundary of a matrix grain is faster than that along the interface. The coarsening resistance behaviour of interpenetrating microstructures has also been observed in the system of alumina/zirconia composites [18]. However, further work is required to elucidate this point.

## 5. Conclusion

The grain growth of Y123 in Y123/Ag composites shows a strong dependence on the amount of silver inclusions and especially on their inter-connectivity. The presence of silver lowers the formation temperature of the liquid phase. Therefore, the grain size of Y123 in the composites is larger than that in pure

TABLE II Coarsening constants,  $K'$ , for coarsening of silver inclusions in Y123/Ag composites

Temperature (°C)	Ag content (%)	$K'$ ( $10^{-24} \text{ m}^4 \text{ min}^{-1}$ )
930	5	0.63
930	10	0.052
930	15	0.013
930	20	0.016

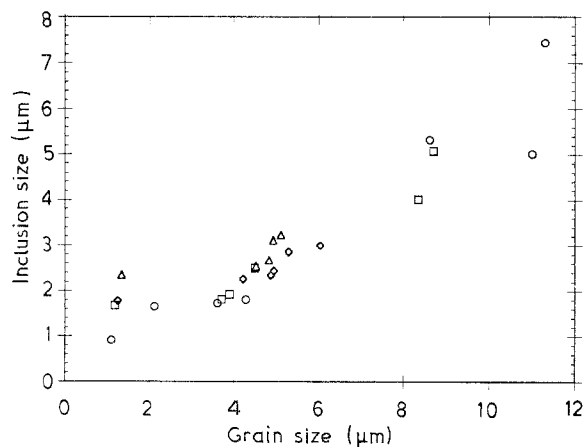


Figure 11 The grain size as a function of inclusion size for all the composites studied in the present study. (○) 5% Ag, (□) 10% Ag, (◇) 15% Ag, (△) 20% Ag.

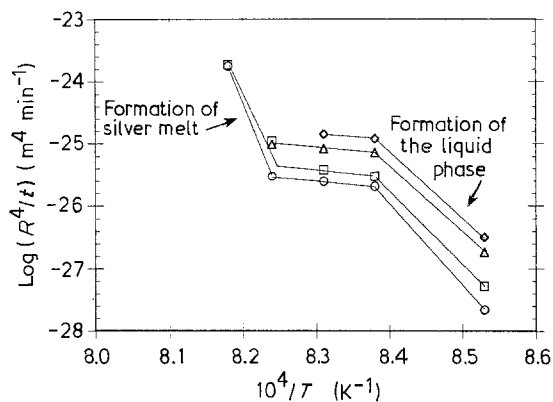


Figure 12 The coarsening constant as a function of sintering temperature. The samples were sintered at the indicated temperatures for 360 min. (○) 5% Ag, (□) 10% Ag, (◇) 15% Ag, (△) 20% Ag.

Y123 at the beginning of sintering. However, as the silver inclusions form an interconnected network, the mass transportation route changed from the grain boundaries of Y123 to the Y123/Ag interfaces. The grain-growth kinetics slowed down significantly.

The silver inclusions in the Y123/Ag composites underwent coarsening during sintering. Because the inclusion size ripened with the grain growth of Y123, it is smaller than the grain size and the inclusions are situated at the junctions of Y123 grains, indicating that the silver inclusions are migrating with the grain boundaries of Y123. The coarsening of silver is therefore a coalescence process. The coarsening rate decreased drastically with increasing silver content. The

presence of Y123 liquid phase can enhance the coarsening rate of silver inclusions. The formation of a silver melt further increased the coarsening rate. The kinetic relationships proposed in the present study may potentially be applied as the principles in the microstructural design of Y123/Ag composites.

## References

1. J. G. BEDNORZ and K. A. MULLER, *Z. Phys.* **B64** (1986) 189.
2. C. W. CHU, P. H. HOR, R. L. MENG, L. GAO, J. Z. HUANG and Y. Q. WANG, *Phys. Rev. Lett.* **58** (1987) 405.
3. R. F. COOK, T. R. DINGER and D. R. CLARKE, *Appl. Phys. Lett.* **51** (1987) 454.
4. R. F. COOK, T. M. SHAW and P. R. DUNCOMBE, *Adv. Ceram. Mater.* **2** (1987) 606.
5. McN N. ALFORD, J. D. BIRCHALL, W. J. CLEGG, M. A. HARMER, K. KENDALL and D. H. JONES, *J. Mater. Sci.* **23** (1988) 761.
6. J. P. SINGH, H. J. LEU, R. E. POEPEL, E. Van VOORHEES, G. T. GOUDEY, K. WINSLEY and S. DONGLU, *J. Appl. Phys.* **66** (1989) 3154.
7. F. YEH and K. WHITE, *ibid.* **70** (1991) 4989.
8. L. S. YEOU and K. W. WHITE, *J. Mater. Res.* **7** (1992) 1.
9. W. H. TUAN and J. M. WU, *J. Mater. Sci.* **28** (1993) 1415.
10. T. H. TIEFEL, S. JIN, R. C. SHERWOOD, M. E. DAVIS, G. W. KAMMLOTT, P. K. GALLAGHER, D. W. JOHNSON Jr, R. A. FASTNACHT and W. W. RHODES, *Mater. Lett.* **7** (1989) 363.
11. D. R. CLARKE, T. M. SHAW and D. DIMOS, *J. Amer. Ceram. Soc.* **72** (1989) 1103.
12. W. WONG-NG, H. F. McMURDIE, B. PARETZKIN, Y. ZHANG, K. K. DAVIS, C. R. HUBBARD, A. L. DRAGOO and J. M. STEWART, *Powder Diff.* **2** (1987) 192.
13. M. W. SHIN, T. M. HARE, A. I. KINGON and C. C. KOCH, *J. Mater. Res.* **6** (1991) 2026.
14. C. T. CHU and B. DUNN, *ibid.* **5** (1990) 1819.
15. C. A. BATEMAN, S. J. BENNISON and M. P. HARMER, *J. Amer. Ceram. Soc.* **72** (1989) 1241.
16. B. W. KIBBEL and A. H. HEUER, *Adv. Ceram.* **12** (1984) 415.
17. I. KAUR, W. GUST and L. KOZMA, "Handbook of Grain and Interphase Boundary Diffusion Data" (Ziegler Press, Stuttgart, 1989).
18. J. D. FRENCH, M. P. HARMER, H. M. CHAN and G. A. MILLER, *J. Amer. Ceram. Soc.* **73** (1990) 2508.

*Received 19 June  
and accepted 24 July 1992*